



Article

# Analytical Model for the Design of Axial Flux Induction Motors with Maximum Torque Density

Georgii Baranov <sup>1</sup>, Alexander Zolotarev <sup>1</sup>, Valerii Ostrovskii <sup>2</sup> and Timur Karimov <sup>3,\*</sup>  
and Alexander Voznesensky <sup>4</sup>

<sup>1</sup> Department of Robotics and Industrial Systems Automation, Saint Petersburg Electrotechnical University "LETI", Professora Popova 5, 197376 Saint Petersburg, Russia; gdbaranov@stud.etu.ru (G.B.); avzolotarev@stud.etu.ru (A.Z.)

<sup>2</sup> Department of Computer-Aided Design, Saint Petersburg Electrotechnical University "LETI", Professora Popova 5, 197376 Saint Petersburg, Russia; vyostrovskii@etu.ru

<sup>3</sup> Youth Research Institute, Saint Petersburg Electrotechnical University "LETI", Professora Popova 5, 197376 Saint Petersburg, Russia

<sup>4</sup> Department of Automation and Control Processes, Saint Petersburg Electrotechnical University "LETI", Professora Popova 5, 197376 Saint Petersburg, Russia; asvoznenskiy@etu.ru

\* Correspondence: tikarimov@etu.ru; Tel.: +7-909-578-82-73

**Abstract:** This article proposes a mathematical model of an axial flux induction motor (AFIM) with one stator and one rotor. The model is based on the expression for the electromagnetic torque, which presents a function of two independent variables: the axial length of the stator core and the flux density in the air gap. This allows calculating the main dimensions of the motor with the highest possible torque density. Thus, developed model is suitable for designing the motor of specified volume with maximum torque, and solving the inverse problem of minimizing the machine volume with the specified torque. The detailed output of the model and the results of the calculations for the low-power engine powered by voltage of 7.35 V (RMS) are given. The results are validated using FEM in ANSYS software: with the outer motor diameter of 0.11 m, the flux density in it reaches 1.2 T.

**Keywords:** expression of electromagnetic torque; design optimization; axial flux induction motor (AFIM); electromagnetic torque density; analytical design; electric vehicles; rotating electrical machines



**Citation:** Baranov, G.; Zolotarev, A.; Ostrovskii, V.; Karimov, T.; Voznesensky, A. Analytical Model for the Design of Axial Flux Induction Motors with Maximum Torque Density. *World Electr. Veh. J.* **2021**, *12*, 24. <https://doi.org/10.3390/wevj12010024>

Received: 3 January 2021

Accepted: 6 February 2021

Published: 11 February 2021

**Publisher's Note:** MDPI stays neutral with regard to jurisdictional claims in published maps and institutional affiliations.



**Copyright:** © 2021 by the authors. Licensee MDPI, Basel, Switzerland. This article is an open access article distributed under the terms and conditions of the Creative Commons Attribution (CC BY) license (<https://creativecommons.org/licenses/by/4.0/>).

## 1. Introduction

The traditional system of designing electrical machines is based on the analysis of a previous experience of their creation, as shown in [1]. With this approach, new samples inherit the advantages and disadvantages of the previous models. Electric machines of the traditional design have a big statistical base accumulated over the previous century of design, allowing for the design of efficient machines of any power. However, when the task is the design of an unusual electrical machine appears, this approach is not possible because there are no statistics available. There are various methods for designing such machines to produce the most effective results.

There are different indicators for evaluating the design quality of an electrical machine: power density [2], the volume torque density and weight torque density [3], the volume and weight of permanent magnets per Newton-meter (for permanent magnet synchronous motor, PMSM) [4], machine price per Newton-meter (for motors [5]), machine price per rated power (for generators [6]), and others [7,8]. When designing any electrical machine, one of the main tasks is obtaining a maximum or minimum one or several of these parameters. When solving problems of maximization of various parameters, different results can be obtained, as shown in [5].

There is still no single mathematical model of an electrical machine, which solves the problem of maximization for at least one of the quality indicators, as stated in [1].

Various soft computing tools such as neural networks [3,9] and metaheuristics are used to solve such problems. The most effective methods for optimizing electrical machines are various matavistic methods. These are computational methods that provide a fairly good approximate solution to the problem in polynomial time.

Metaheuristics includes several methods, such as Ant Colony, evolutionary optimization, and genetic algorithms [5,10–12] as well as some combinations of them.

For example, L.S. Batista et al. in [13] use the Ant Colony metaheuristic method to solve the problems of optimization of the Interior Permanent Magnet Machine, namely, the task of minimizing the volume of permanent magnets per Newton-meter and the problem of improving the shape of the MMF curve in the air gap. The result of this study is two different topological forms of rotor design, providing solutions to two set tasks. Both structures are technologically feasible. However, a great disadvantage of the developed technique is that it is aimed only at optimizing the shape of the rotor and shape of stator slots but the stator core is not optimized.

A.C.F. Mamede and J.R. Camacho in [14] use an evolutionary optimization algorithm to maximize electromagnetic torque per total volume of a single-phase switched recovery machine and to decrease electrical losses in copper. The main parameter of motors of similar design is the angle of rotor and stator arc. The result of this study is the design of an engine having the maximum possible torque in a given volume. However, as with any other metaheuristic method, the result was achieved through repeated effort. In this case, the result was achieved in 50 iterations, but it should be noted that the work was carried out through the modernization of the already existing engine, i.e., the initial data for starting the evolutionary algorithm were known at the beginning. It would take many more iterations to calculate an engine without initial data.

P. Vrtic and M. Vrazic in [5] apply genetic algorithms to the optimum design of the axial flux permanent magnet synchronous motor with two stators. Several optimization tasks were solved in this work: (1) maximized weight torque density, (2) maximized volume torque density, (3) minimized mass of PMs per Newton-meter, (4) minimized volume of PMs per Newton-meter, and (5) minimized machine price per Newton-meter. The result of the work was five completely different electric motor designs, solving different tasks. Each of the tasks required about 4000 iterations. With the use of computer equipment available to the authors, the calculation of each iteration took 145 s, and the complete calculation of the engine design took about 13.5 h.

T. Raminosa and B. Blunier in [11] also use genetic algorithms to upgrade a high-speed switched reluctance machine in an air compressor.

In addition, there are combined optimization techniques that use neural networks and various metaheuristic algorithms for design. For instance, S. Meo and A. Zohoori in [9] use a combination of the metaheuristic method “particle swarm optimization” and four neural networks to optimize a permanent magnet flux switching generator for a low-power wind turbine, namely, to minimize the weight and price of the generator, as well as to improve the harmonic composition of the induced voltage. Neural networks are designed to model complex relationships between weight, volume, cost, and the harmonic distortion factor. The metaheuristic algorithm serves to find the best solution in the entire search space. FEM calculations were used to train neural networks. Such combined methods are very effective, however, training neural networks, as well as working out all iterations required a metaheuristic algorithm which takes a long time and computational power.

The main contribution of an article is that we propose a motor design procedure aimed for torque density optimization. Such a conception was not proposed before in any of the publications we know. Currently, the most common optimization approaches are based on metaheuristics or the application of neural networks. They provide an optimal solution, with a high degree of accuracy, but they require multiple iterations to be processed. This requires a lot of processing power and a lot of time. This article proposes a simplified mathematical model of an electric machine, allowing to design electric motors in one iteration with the maximum possible torque density. With this model, the Axial

Flux Induction Machine (AFIM) with a short-circuited rotor will be designed in operation. However, this technique can be adapted to any type of a motor.

## 2. Materials and Methods

In the paper [15], M.N. Benallal gives the basic principles of the model of an induction motor proposed by M.A. Vaganov. The optimal value of the inner diameter of the stator and flux density in the air gap can be obtained as a result of using this model. Optimization is performed with a constant value of the outer diameter and axial length of the stator steel package. An optimum in the indicated variables ensures the maximum value of the electromagnetic torque. Thus, the model allows us to obtain the maximum value of the electromagnetic torque for a given volume of the machine. However, this model is proposed for the classic performance of an induction motor. It is necessary to formulate it for an axial flux induction motor.

### 2.1. Thought Experiment

The principle of this optimization can be illustrated by a simple thought experiment. Suppose that a machine occupies a fixed volume, i.e., its outer diameter  $D_o$  and the total axial length  $L$  are unchanged. If, within the framework of a constant axial length  $L$ , the length of the stator core is changed by  $l_1$ , then the length of the rotor core will be determined by the expression  $l_2 = L - l_1$ .

Further, we assume that if we increase the length of the stator core  $l_1$  (as in Figure 1a) in the limit to the total axial length  $L$ , then the length of the steel stack of the rotor  $l_2$  tends to zero, and a motor of this design will develop an electromagnetic torque that also tends to zero. On the contrary, if the stator core length  $l_1$  (as in Figure 1c) is reduced to zero, then the length of the rotor core  $l_2$  will tend to the total length of the machine  $L$ , and the torque developed by such a machine will also tend to zero.

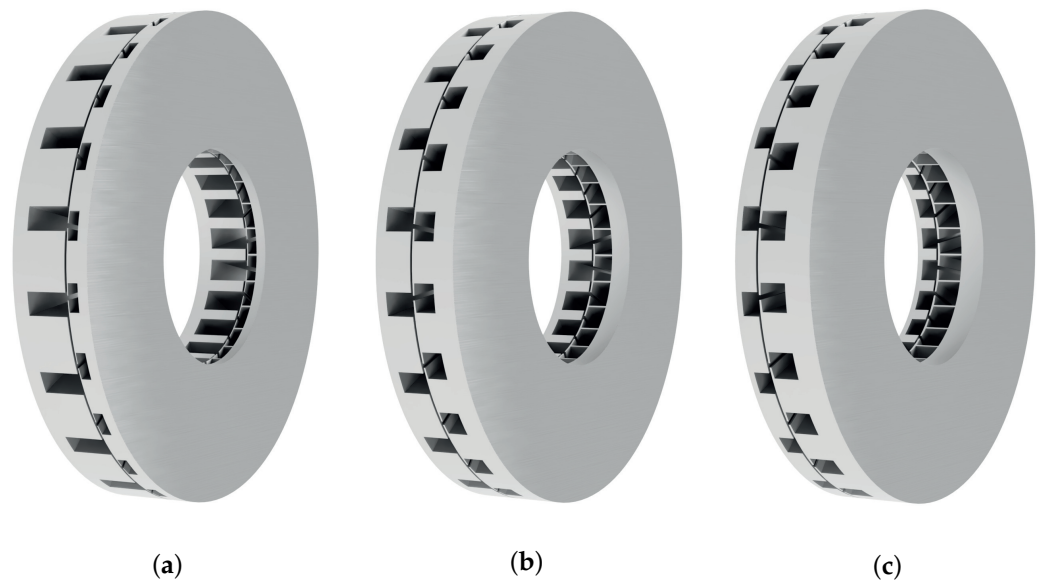


**Figure 1.** Illustration of a thought experiment. (a) Illustration of the Axial Flux Induction Machine (AFIM) in which the stator occupies 80% of the axial length, (b) the stator occupies 50% of the axial length, and (c) the stator occupies 30% of the axial length.

Based on Rolle's theorem, the electromagnetic torque as a function of the length of the stator core must have at least one extremum in the considered interval. Thereby, the basis for the mathematical model is the expression of the electromagnetic torque of the induction motor:

$$T_{em} = \frac{m_1 U_1^2}{\omega_s} \frac{R_2'/s}{(R_1 + c_1 R_2'/s)^2 + (X_1 + c_1 X_2')^2} \quad (1)$$

where  $T_{em}$  is electromagnetic torque [Nm];  $m_1$ —a number of stator phases;  $\omega_s$ —electrical angular velocity;  $U_1$ —the phase voltage of the stator [V, RMS];  $R_1$ —stator resistance [Ohm];  $R_2'$ —the resistance of the rotor referred to the stator [Ohm];  $X_1$ —stator reactance [Ohm];  $X_2'$ —the rotor reactance referred to the stator [Ohm]; and  $c_1$ —coefficient taking into account voltage drop at full resistance of stator winding.

## 2.2. Model Expression Generation

Equation (1) needs to be converted. It is both multiplied and divided by the square root of the product of the phase resistance of the stator and the phase resistance of the rotor referred to the stator:

$$T_{em} = \frac{m_1 U_1^2}{\omega_s \sqrt{R_1 R_2'}} \sqrt{R_1 R_2'} \frac{R_2'/s}{(R_1 + c_1 R_2'/s)^2 + (X_1 + c_1 X_2')^2} \quad (2)$$

The phase voltage  $U_1$  can be represented as the product of the electromotive force (EMF)  $E_{10}$  [V, RMS] of the self-induction of the stator winding and the coefficient  $c_1$  taking into account the voltage drop on the winding resistance.

$$U_1 = E_{10} c_1 \quad (3)$$

In turn,  $E_{10} = \pi \sqrt{2} f_1 k_w W_1 \Phi_m$ , where  $f_1$  is the frequency of the voltage of the stator winding;  $W_1$ —the number of turns connected in series of the stator winding phase;  $\Phi_m$ —magnetic flux [Wb]; and  $k_w$ —winding factor.

If the active length of the stator conductors is taken to be equal to  $l_1 = (D_o - D_i)/2$  and the pole pitch of the stator is equal to  $\tau_p = \pi(D_o + D_i)/2$ , then the amplitude of the rotating magnetic flux of mutual flux density in the air gap is

$$\Phi_m = \frac{2}{\pi} \tau_p l_1 B_\delta = B_\delta \frac{(D_o^2 - D_i^2)}{4p} \quad (4)$$

where  $D_i$  is inner diameter [m];  $D_o$ —outer diameter [m];  $\tau_p$ —pole pitch [m];  $B_\delta$ —magnetic flux density in air gap [T]; and  $p$ —the number of pole pairs.

Of greatest interest in Equation (2) is the first coefficient. For the further formation of the expression of the mathematical model, it is necessary to obtain expressions for the resistances of the rotor and the stator windings, as well as expressions for the cross-sectional area of the slots of the stator and rotor.

### 2.2.1. Stator Resistance

The phase resistance can be defined as the ratio of the doubled number of turns of the winding  $W_1$  multiplied by the average length of the half-turn of the coil  $l_{1ht}$  and the temperature factor  $k_{\theta 1}$  to the specific electrical conductivity  $\gamma_1$  [S/m] of the winding material and the cross-sectional area of the winding conductor  $q_{a1}$  [m<sup>2</sup>].

$$R_1 = \frac{2W_1 l_{1ht} k_{\theta 1}}{\gamma_1 q_{a1}} \quad (5)$$

In the process of generating an expression for the average half-turn of the stator winding, it must be taken into account that the stator has two coil spans of different lengths along the outer diameter of the stator  $\pi D_o k_p / 4p$  and along the inner diameter of the stator  $\pi D_i k_p / 4p$ :

$$l_{1ht} = \frac{k_{ew}}{2} (D_o - D_i) + \frac{\pi}{4p} (D_o + D_i) k_p \quad (6)$$

where the radial length factor of the end winding  $k_{ew}$  shows the radial length of the end winding in units of the length of the active part and  $k_p$  is pitch factor.

We introduce the notation

$$k_D = \frac{D_o + D_i}{D_o - D_i} \quad (7)$$

and transform Equation (6):

$$l_{1ht} = k_{1*} \frac{D_o - D_i}{2} \quad k_{1*} = k_{ew} + \frac{\pi k_p k_D}{2p}, \quad (8)$$

where coefficient  $k_{1*}$  describes the length of the end winding.

Next, we transform Equation (5) for the resistance of the stator winding, taking into account Equation (8):

$$R_1 = \frac{W_1 (D_o - D_i) k_{1*} k \vartheta}{\gamma_1 q_{a1}}. \quad (9)$$

### 2.2.2. Rotor Cage Resistance

According to the work in [16], the resistance of the short-circuited rotor winding related to the stator winding of a conventional cylindrical induction motor is determined by the expression:

$$R'_2 = \frac{4m_1 (k_w W_1)^2}{z_2} \left( R_{bar} + \frac{R_{ring}}{2 \sin^2 \frac{\pi p}{z_2}} \right), \quad (10)$$

where  $z_2$  is the number of the rotor slots.

The length of the bar is defined as  $l_{bar} = (D_o - D_i)/2$ . Therefore, the resistance of the rod is

$$R_{bar} = \frac{k_{\vartheta 2} (D_o - D_i)}{2 \gamma_2 q_{bar}},$$

where  $k_{\vartheta 2}$  is the thermal factor of the rotor;  $\gamma_2$ —conductivity of rotor conductors [S/m]; and  $q_{bar}$ —area of the rotor rods [m<sup>2</sup>].

In the short-circuited winding of the rotor of the end induction motor there must also be two short-circuited rings: the outer ring with diameter  $D_o$  and the inner with diameter  $D_i$ . Without significant error, the diameters of the rings can be equal to the outer and inner diameters of the rotor core, respectively, and then

$$R_{ring} = \frac{\pi k_{\vartheta 2}}{z_2 \gamma_2 q_{ring}} (D_o + D_i),$$

where  $q_{ring}$  is area of short-circuited rings [m<sup>2</sup>].

Equation (10) can be transformed as

$$R'_2 = \frac{4m_1 (k_w W_1)^2}{z_2} \frac{k_{\vartheta 2}}{\gamma_2 q_{bar}} \left( \frac{D_o - D_i}{2} + \frac{\pi (D_o + D_i) q_{bar}}{z_2 q_{ring}} \frac{1}{2 \sin^2 \frac{\pi p}{z_2}} \right). \quad (11)$$

The cross-sectional areas of the bar  $q_{bar}$  and the short-circuit ring  $q_{ring}$  can be represented by the ratio of the currents in them  $I_{bar}$  and  $I_{ring}$  to the corresponding current densities  $J_{bar}$  and  $J_{ring}$ .

The decrease in current density in the short-circuited rotor rings relative to the current density in the rods (to improve the cooling conditions of the rods) can be taken into account

using the coefficient  $k_J = I_{ring}/I_{bar}$ . Thus, the ratios  $q_{bar}$  and  $q_{ring}$  can be compiled taking into account the fact that  $I_{bar}/I_{ring} = 2 \sin(\pi p/z_2)$  according to the work in [16].

$$\frac{q_{bar}}{q_{ring}} = \frac{I_{bar}}{I_{ring}} \frac{J_{ring}}{J_{bar}} = 2 k_J \sin(\pi p/z_2)$$

Substitute this in Equation (11).

$$R'_2 = \frac{2 m_1 (k_w W_1)^2 k_{\theta 2}}{\gamma_2 z_2 q_{bar}} \left( (D_o - D_i) + \frac{k_J \pi (D_o + D_i)}{z_2 \sin(\pi p/z_2)} \right)$$

For the final form of expression for  $R'_2$ , (7) should be taken into account.

$$R'_2 = \frac{2 m_1 (k_w W_1)^2 k_{\theta 2} k_{2*}}{\gamma_2 z_2 q_{bar}} (D_o - D_i), \quad k_{2*} = 1 + \frac{\pi k_J k_D}{z_2 \sin(\pi p/z_2)} \quad (12)$$

### 2.2.3. Slot Cross-Sectional Area

The expression for the stator slot area  $Q_{s1}$  [m<sup>2</sup>] is the product of the total number of stator winding conductors  $N_{c1} = 2 W_1 m_1$  and the cross-sectional area of the conductor without insulation  $q_{a1}$ , taking into account the space factor for copper  $k_{Cu}$ .

$$Q_{s1} = \frac{N_{c1} q_{a1}}{k_{Cu}} = \frac{2 W_1 m_1 q_{a1}}{k_{Cu}} \quad (13)$$

A similar expression can be written for the rotor, taking into account the fact that with a squirrel cage rotor, only one bar with a cross section  $q_{bar}$  is located in the slot. Then, the total area  $Q_{s2}$  [m<sup>2</sup>] is required to place  $z_2$  rods in it with a space factor for aluminum  $k_{Al}$ .

$$Q_{s2} = \frac{z_2 q_{bar}}{k_{Al}} \quad (14)$$

### 2.2.4. General Model Expression

Now Equation (2) can be transformed by substituting Equations (3), (4), (9), and (12), taking into account (13) and (14):

$$T_{em} = \frac{\pi f_1 k_w c_1^2 \sqrt{\gamma_1 \gamma_2 k_{Cu} k_{Al}} (D_o + D_i) (D_o^2 - D_i^2) B_\delta^2 \sqrt{Q_{s1} Q_{s2}}}{32 \sqrt{k_{\theta 1} k_{\theta 2}} \sqrt{k_{1*} k_{2*}}} \frac{1}{p} F. \quad (15)$$

The last two coefficients of Equation (2) can be denoted as a "parametric factor"  $F$ .

$$F = \sqrt{R_1 R'_2} \frac{R'_2/s}{(R_1 + c_1 R'_2/s)^2 + (X_1 + c_1 X'_2)^2} \quad (16)$$

The first factor of (15) is a generalized coefficient  $k_F$ , which includes several quantities that are constant or almost constant, i.e., their numerical values are known or set in accordance with the task for engine design.

$$k_F = \frac{\pi f_1 k_w c_1^2 \sqrt{\gamma_1 \gamma_2 k_{Cu} k_{Al}}}{32 \sqrt{k_{\theta 1} k_{\theta 2}}} \quad (17)$$

The remaining part of (15) can be called a "functional factor"  $F_M$  describing the longitudinal-transverse geometry of an AFIM. This expression will be further transformed taking into account the specific shape of the slot of the stator and rotor.

$$F_M = \frac{(D_o + D_i) (D_o^2 - D_i^2) B_\delta^2 \sqrt{Q_{s1} Q_{s2}}}{\sqrt{k_{1*} k_{2*}}} \frac{1}{p} \quad (18)$$

Moreover, the equation of the model can be written as

$$T_{em} = k_F F_M F. \quad (19)$$

### 2.2.5. Area of Rectangular Slots

For simplicity, rectangular open slots on the stator are considered. The width of the slot  $b_{s1}$  can be determined from the expression for the area of the slot in the plane of the air gap  $\tilde{Q}_{s1}$ . If we make the assumption that the arcs of the circles that limit the slot along the outer and inner surfaces of the stator core are equal to the corresponding chords, then  $b_{s1} = \tilde{Q}_{s1}/((D_o - D_i)/2)$ .

In its turn, the stator slot area can be found as the difference between the area of the tooth pitch and the tooth  $Q_{s1} = Q_\tau - Q_{t1}$ . The area corresponding to the tooth pitch of the stator (hatched area 1 in Figure 2, see also isometric view in Figure 3) is defined as

$$Q_\tau = \frac{\pi D_o^2}{4} \frac{2\pi/z_1}{2\pi} - \frac{\pi D_i^2}{4} \frac{2\pi/z_1}{2\pi} = \frac{\pi}{4z_1} (D_o^2 - D_i^2),$$

where  $z_1$  is the number of the stator slots.

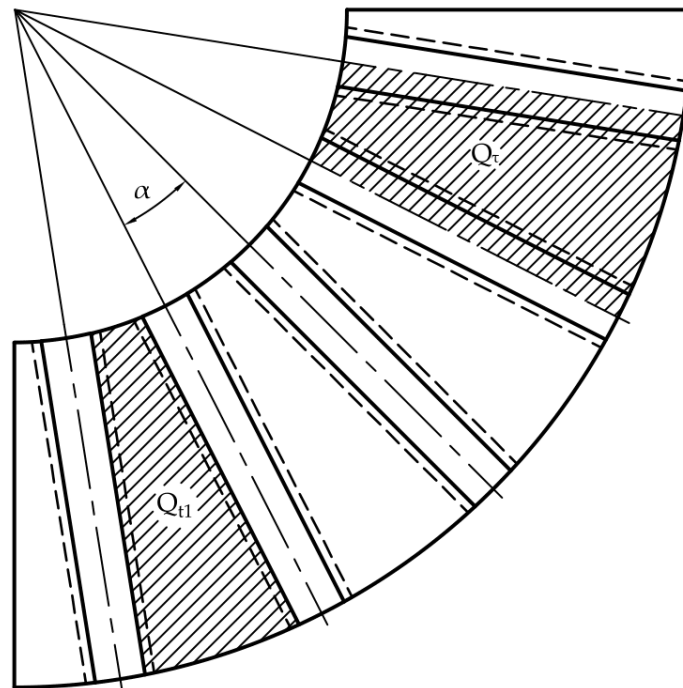


Figure 2. Stator tooth zone in the plane of the air gap.

If flux density in the air gap  $B_\delta$  is evenly distributed within the tooth pitch, then the magnetic flux corresponding to the tooth pitch  $\Phi_{t1} = Q_\tau B_\delta = Q_t B_t k_{Cu}$ .

The dependence of the area of tooth pitch and tooth can be found as

$$Q_{t1} = Q_\tau \frac{B_\delta}{B_{t1} k_{Fe}},$$

where  $k_{Fe}$  is space factor for iron;  $B_{t1}$ —magnetic flux density in stator teeth [T].

Then, the tooth pitch and stator slot area will be written as

$$Q_\tau = \frac{\pi}{4z_1} (D_o^2 - D_i^2) \frac{B_\delta}{B_{t1} k_{Fe}},$$

$$\tilde{Q}_{s1} = Q_\tau - Q_{t1} = \frac{\pi}{4z_1} (D_o^2 - D_i^2) \left(1 - \frac{B_\delta}{B_{t1} k_{Fe}}\right).$$

Now it is possible to determine the width of the stator tooth.

$$b_{s1} = \frac{\tilde{Q}_{s1}}{(D_o - D_i)/2} = \frac{\pi}{2z_1} (D_o + D_i) \left(1 - \frac{B_\delta}{B_{t1} k_{Fe}}\right) \quad (20)$$

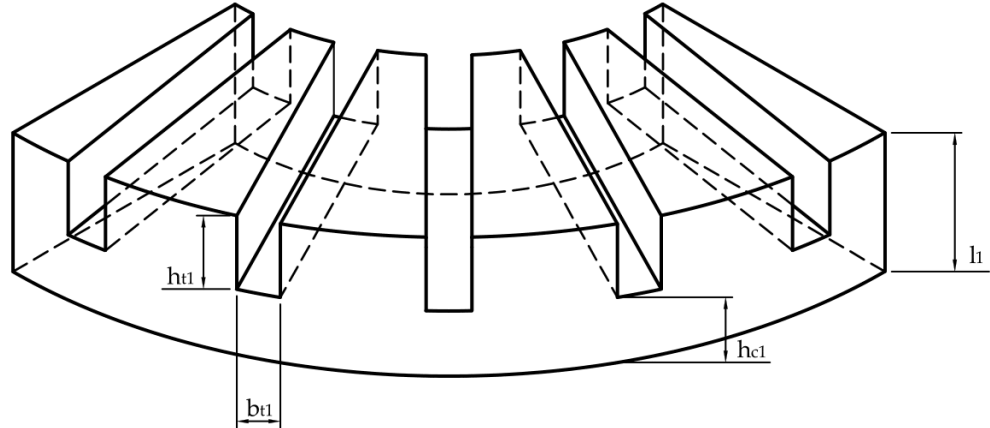


Figure 3. Stator teeth in isometric.

To find the height of the stator core  $h_{c1}$  and tooth  $h_{s1}$ , it is necessary to convert the expression for the amplitude of the magnetic flux. It is desirable that only half of the magnetic flux passes through the core. In such a case, the expression for the magnetic flux (Equation (4)) is written as

$$\Phi_m = B_\delta \frac{(D_o^2 - D_i^2)}{4p} = B_{c1} \frac{(D_o - D_i)}{2} h_{c1} k_{Fe},$$

where  $B_{c1}$  is magnetic flux density in stator core [T].

After the magnetic flux conversion, it is possible to find the stator core thickness as well as the height of the stator slots.

$$h_{c1} = \frac{(D_o + D_i)}{4p} \frac{B_\delta}{B_{c1} k_{Fe}} \quad (21)$$

The height of the stator tooth can be determined as the difference between the thickness of the stator steel stack and the thickness of the stator core.

$$h_{s1} = l_1 - h_{c1} = l_1 - \frac{(D_o + D_i)}{4p} \frac{B_\delta}{B_{c1} k_{Fe}} \quad (22)$$

In the simplest case, it can be assumed that the rotor slots are also rectangular, and the outer and inner diameters of the rotor and stator are equal ( $D_{o1} = D_{o2} = D_o$ ;  $D_{i1} = D_{i2} = D_i$ ). Then, the geometric dimensions of the slots and core of the rotor can be found in the same way as the slots and core of the stator, i.e., Equations (20)–(22) simply change indexes from 1 to 2.

### 2.2.6. Relative Dimensions

In order to obtain a general solution to this problem, we will introduce a system of relative dimensions, taking as the basic total axial length of the engine  $L$ . Under this condition, the main relative dimensions of the engine can be written as  $D_{o*} = D_o/L$ ,  $D_{i*} = D_i/L$ ,  $l_{1*} = l_1/L$ .

In such a case, the geometric dimensions of the stator slots can be converted as

$$b_{s1} = L \left( \frac{\pi}{2z_1} (D_{o*} + D_{i*}) \left(1 - \frac{B_\delta}{B_{t1} k_{Fe}}\right) \right), \quad (23)$$

$$h_{s1} = L(l_{1*} - \frac{(D_{o*} + D_{i*})}{4p} \frac{B_{\delta}}{B_{c1}k_{Fe}}). \quad (24)$$

The total area of all stator slots can be written as:

$$Q_{s1} = Z_1 b_{s1} h_{s1} = L^2 k_{s1}, \quad (25)$$

$$k_{s1} = \frac{\pi}{2} (D_{o*} + D_{i*}) (1 - \frac{B_{\delta}}{B_{t1}k_{Fe}}) (l_{1*} - \frac{(D_{o*} + D_{i*})}{4p} \frac{B_{\delta}}{B_{c1}k_{Fe}}).$$

The axial length of the rotor core can be written as  $l_2 = L - l_1 - \delta$ , where  $\delta$  is thickness of air gap. Provided that the rotor slots are also rectangular, their total area is written similarly.

$$Q_{s2} = Z_2 b_{s2} h_{s2} = L^2 k_{s2} \quad (26)$$

$$k_{s2} = \frac{\pi}{2} (D_{o*} + D_{i*}) (1 - \frac{B_{\delta}}{B_{t2}k_{Fe}}) (l_{1*} - \frac{(D_{o*} + D_{i*})}{4p} \frac{B_{\delta}}{B_{c2}k_{Fe}})$$

Given (25) and (26), the Equation (18) is written as

$$F_M = \frac{(D_{o*} + D_{i*})(D_{o*}^2 - D_{i*}^2)L^5 B_{\delta}^2 \sqrt{K_{s1} K_{s2}}}{\sqrt{k_{1*} k_{2*}}} \frac{1}{p}.$$

This conversion allows us to rewrite the expression for the electromagnetic torque in relative units:

$$T_{em} = k_F F_{M*} FL^5, \quad (27)$$

$$F_{M*} = \frac{(D_{o*} + D_{i*})(D_{o*}^2 - D_{i*}^2)B_{\delta}^2 \sqrt{K_{s1} K_{s2}}}{\sqrt{k_{1*} k_{2*}}} \frac{1}{p}. \quad (28)$$

### 3. Results

#### 3.1. Calculation Example

##### 3.1.1. Design Setup

As mentioned in Section 1, the developed mathematical model allows us to design optimal AFIM by setting some initial data. In order to illustrate the developed method, we solve the problem of AFIM design with maximum possible electromagnetic torque density in the specified volume, i.e., with hard-limited axial length and outer diameter of stator and rotor steel packages. However, note that by using the same patterns and equations, it is possible to solve the inverse problem, i.e., the task of building an engine with specified torque in minimum volume. In any case, the result of this technique is an electric motor with the maximum possible torque density.

The results below will be for solving the problem of designing a low-voltage AFIM with four pole pairs. Such motors can be widely used in small electric transport [17–20], for example, in electric bicycles or electric kick scooters, i.e., in devices with severely limited consumption. Initial data for the design are given in Table 1.

##### 3.1.2. Applications of the Analytical Model

The most significant variables defining all the characteristics of the machine are the axial length of the stator, which determines the relationship between the stator and the rotor (see Section 2.1) and flux density in the air gap. These variables mainly determine the value of the electromagnetic torque (19). As these variables are independent of each other, one can find the extremes of this expression from them.

It should be noted that the values of the parametric factor (16) and generalized coefficient (17) do not depend on these variables, i.e., extremes of electromagnetic torque are at the same points as extremes of the expression of functional factor (18).

After substituting the initial data in the model expression, the following dependencies were obtained (Figure 4).

**Table 1.** Initial data of design process.

Designation	Name	Value	Unit
U	Line voltage, RMS	7.35	V
$U_{max}$	Maximum line voltage	36	V
f	Rated frequency	50	Hz
$f_{max}$	Maximum frequency	100	Hz
$D_o$	Outer diameter	0.11	m
$D_i$	Inner diameter	0.05	m
L	Total thickness	0.03	m
$m_1$	The number of phases	3	-
p	The number of pole pairs	4	-
q	The number of slots per pole and phase	1	-
$y_1$	Step of span in slot pitches	3	-
$z_2$	The number of rotor slots	32	-
$k_{Cu}$	Space factor for copper	0.5	-
$k_{Fe}$	Space factor for iron	0.98	-
$k_{Al}$	Space factor for aluminum	0.97	-
$k_{\theta 1}$	Thermal factor	1.32	-
$\delta$	Thickness of air gap	1	mm
$k_m$	Overload capability	2	-
$B_{c1}$	Inductance of stator core	1.4	T
$B_{c2}$	Inductance of rotor core	1.3	T
$B_{t1}$	Inductance in stator teeth	1.8	T
$q_{a1}$	Cross-section of 1 conductor	$2.8 \times 10^7$	m <sup>2</sup>

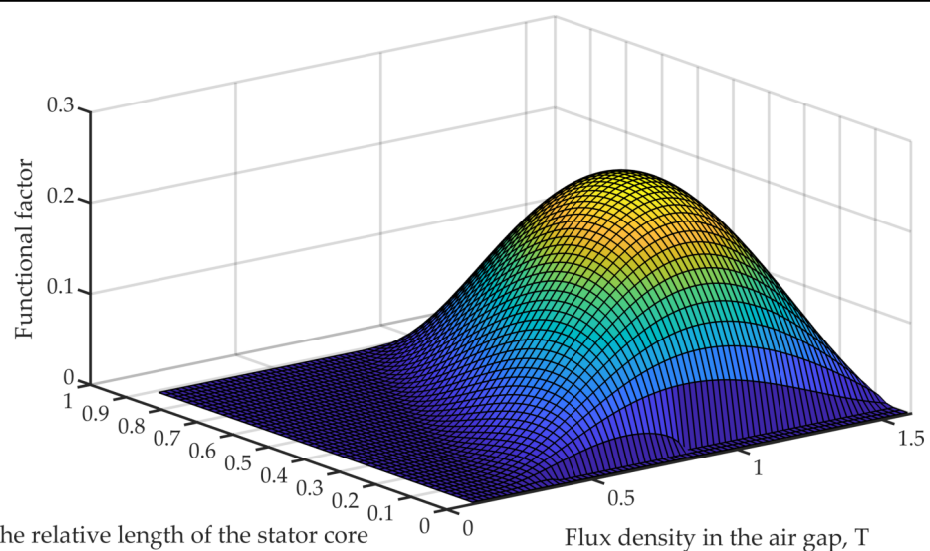


**Figure 4.** Constraints determining electromagnetic torque.

From Figure 4, it can be seen that the electromagnetic torque takes the maximum value at the following values of variables:  $l_1 = 13.9$  mm;  $B_\delta = 1.13$  T. These values provide the maximum torque density in the designed engine.

Rotor steel pack thickness can be found as the difference of total engine thickness, stator steel pack thickness, and air gap values.

$$l_2 = L - l_1 - \delta = 15.1 \text{ mm} \quad (29)$$

Substituting in Equations (22) and (20) initial data and obtained values, dimensions of stator and rotor slots can be found geometrically. The following results were obtained  $h_{s1} = 5.4$  mm;  $h_{s2} = 6.3$  mm;  $b_{s1} = 3.7$  mm;  $b_{s2} = 2.8$  mm. After substitution of all obtained values in all model expressions, the maximum possible value of electromagnetic torque was obtained  $T_{em} = 0.84$  Nm.

### 3.2. Validation of Calculated Results

The calculated engine was validated by using FEM, the analytical method based on Maxwell's equations, and the measured torque. The external view of the designed engine is shown in Figure 5.

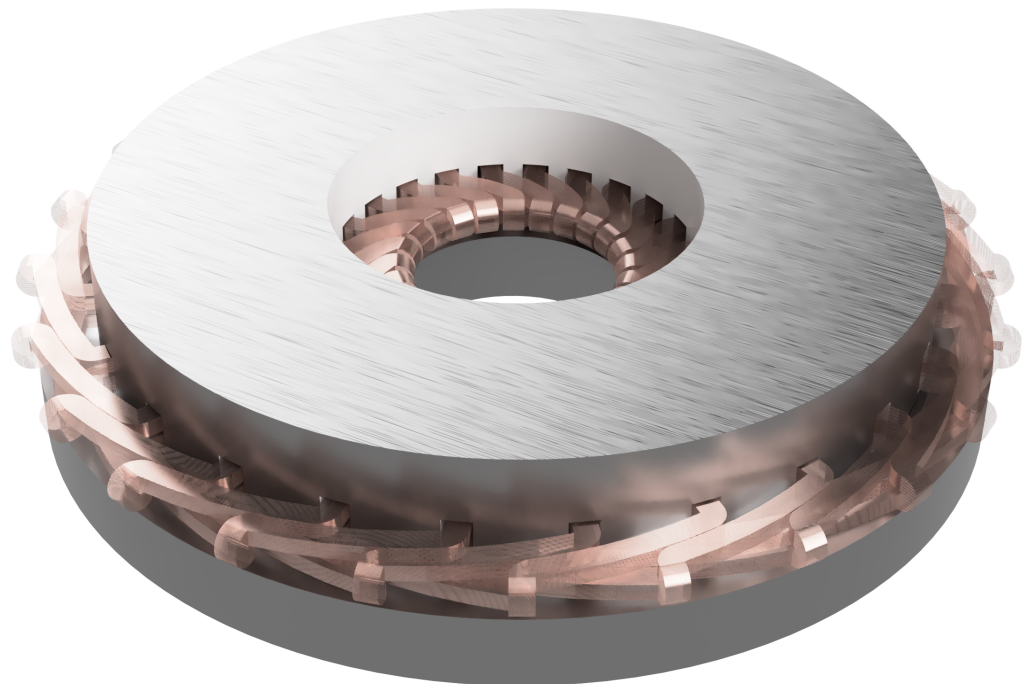


**Figure 5.** Engine model in isometry.

Electromagnetic torque is presented in Figure 6, in the steady state electromagnetic torque pulsations are observed, however this is normal for AFIM [21]. The pattern of magnetic flux density in the air gap is presented in Figure 7.

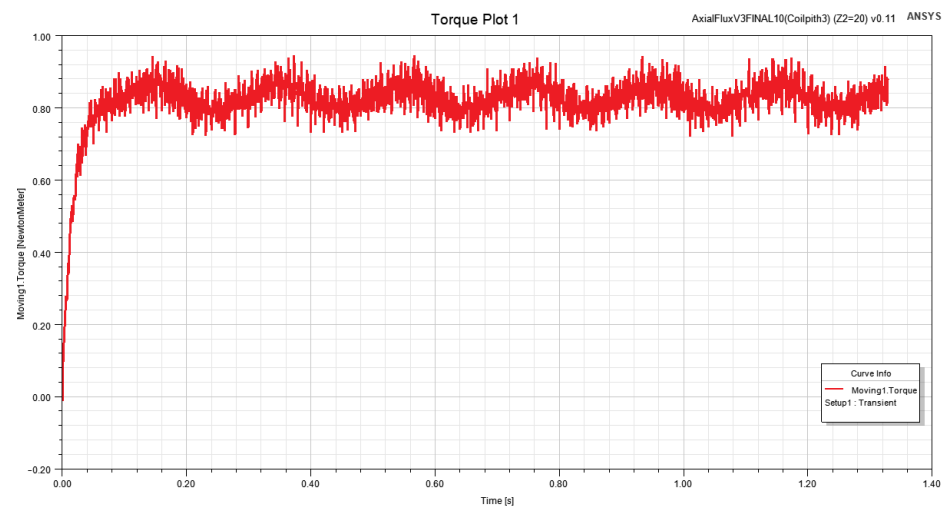


Figure 6. Electromagnetic torque.

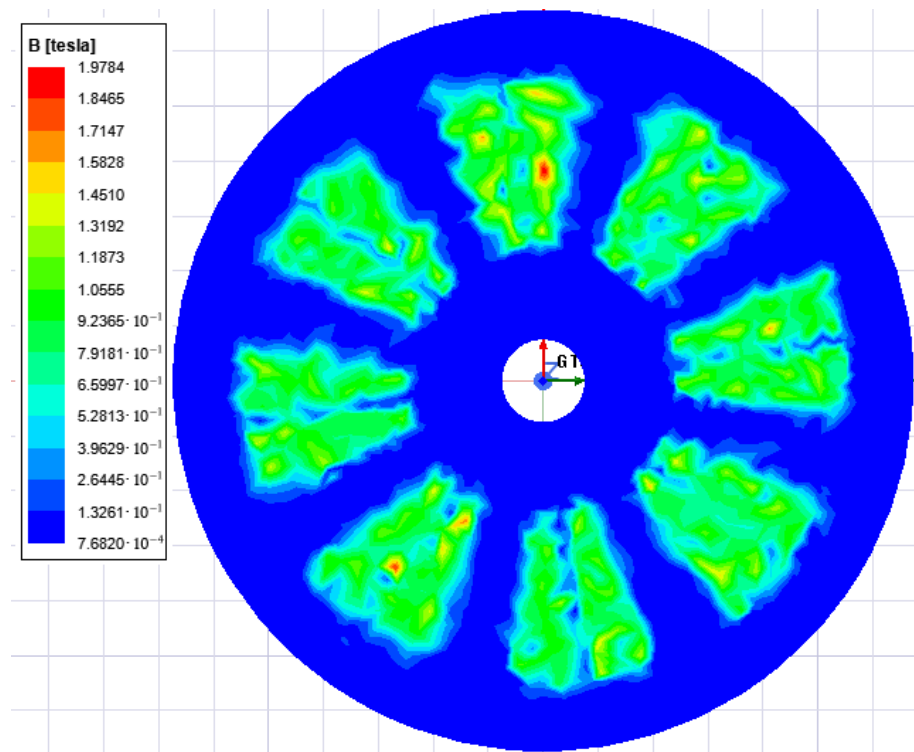


Figure 7. Magnetic flux density in air gap.

Figure 7 clearly shows four pairs poles of motor; in addition, it is clear that the amplitude of magnetic flux density in the air gap reaches 1.1–1.2 T, which corresponds to the optimal value of the amplitude of magnetic flux density in the air gap (Figure 4). For AFIM with one stator and one rotor, the amplitude of magnetic flux density in air gap usually does not exceed 1.2 T, as shown in [22,23].

#### 4. Discussion

This article shows the possibility of optimizing an electric machine in a closed volume. Classic electric machine models, such as those based on the output equation [16], optimize the machine for the inner diameter of the stator without controlling its outer diameter. A distinctive feature of our technique is taking into account the external dimensions of

the machine and optimizing the dimensions of the stator and rotor already inside this given volume.

In our opinion, another important scientific result of this work is obtaining a mathematical model of the motor as a design object. This makes it possible to conduct research on the influence of various design parameters on the characteristics of an electric machine. Note that for a more reliable description of the electric machine, the model should be improved. The model must be supplemented with characteristics of steel magnetization, heat transfer and heat removal processes, the ability to set an efficiency class, and other additional functions.

## 5. Conclusions

The article proposes an analytical model of AFIM, with which it is possible to design an electric motor with the maximum possible electromagnetic torque density. By analyzing the expression of the electromagnetic torque, the model allows us to obtain an optimal value of magnetic flux density in the air gap, as well as geometric parameters of the motor, namely, axial lengths of the stator and rotor steel packs and the height and width of the stator and rotor slots.

In the articles considered in the introduction, similar results are achieved through various soft computing techniques, namely, neural networks and metaheuristic algorithms. A common disadvantage of these methods is that they require working out multiple iterations to achieve the goal. It takes a lot of time and computing power for processing these iterations. The model presented in this article allows us to solve the problem in a single iteration.

To illustrate the operability of the model, we calculated a small low-voltage AFIM with four pairs of poles. In addition, the designed engine was validated using the FEM.

This model not only provides an algorithm for calculating the engine for a single iteration, but is also a valuable research tool. The influence of various parameters on the characteristics of an electric machine can be obtained in the context of its analysis. Therefore, in the following publications, the analysis of the influence of the number of poles and other parameters on the characteristics of the machine will be checked.

**Author Contributions:** Conceptualization, G.B. and T.K.; data curation, V.O.; formal analysis, G.B. and A.V.; investigation, A.Z. and A.V.; methodology, G.B.; project administration, G.B. and T.K.; resources, A.Z., T.K., and A.V.; software, A.Z. and T.K.; supervision, G.B.; validation, V.O. and A.V.; visualization, A.Z. and V.O.; writing—original draft, G.B.; writing—review and editing, V.O. and T.K. All authors have read and agreed to the published version of the manuscript.

**Funding:** This research received no external funding.

**Conflicts of Interest:** The authors declare no conflicts of interest.

## Abbreviations

The following abbreviations are used in this manuscript:

AFIM	Axial flux induction motor
FEM	Finite element method
$p$	the number of pole pairs
$T_{em}$	electromagnetic torque [Nm]
$m_1$	number of stator phases
$U_1$	the phase voltage of the stator [V], RMS
$\omega_s$	electrical angular velocity
$R_1$	stator resistance [Ohm]
$R'_2$	the resistance of the rotor referred to the stator [Ohm]
$c_1$	Coefficient taking into account voltage drop at full resistance of stator winding
$X_1$	stator reactance [Ohm]

$X'_2$	the rotor reactance referred to the stator [Ohm]
$E_{10}$	electromotive force (emf) [V], [RMS]
$W_1$	the number of series-connected turns of the stator winding
$\Phi_m$	magnetic flux [Wb]
$D_i$	inner diameter [m]
$D_o$	outer diameter [m]
$\tau_p$	pole pitch [m]
$l_1$	the stator thickness [m]
$l_2$	the rotor thickness [m]
$\delta$	thickness of air gap [m]
$L$	the total thickness of the machine [m]
$B_\delta$	magnetic flux density in air gap [T]
$B_{t1}$	magnetic flux density in stator teeth [T]
$B_{t2}$	magnetic flux density in rotor teeth [T]
$B_{c1}$	magnetic flux density in stator core [T]
$B_{c2}$	magnetic flux density in rotor core [T]
$k_{\theta 1}$	the thermal factor of the stator
$k_{\theta 2}$	the thermal factor of the rotor
$\gamma_1$	conductivity of stator conductors [S/m]
$\gamma_2$	conductivity of rotor conductors [S/m]
$q_{a1}$	area of the stator conductor [m <sup>2</sup> ]
$q_{bar}$	area of the rotor rods [m <sup>2</sup> ]
$q_{ring}$	area of short-circuited rings [m <sup>2</sup> ]
$J_{bar}$	current density of rotor rods [A/m <sup>2</sup> ]
$J_{ring}$	current density of short-circuited rings [A/m <sup>2</sup> ]
$Q_\tau$	the area of the coil pith [m <sup>2</sup> ]
$\tilde{Q}_{s1}$	the area of the stator slot [m <sup>2</sup> ]
$Q_{s1}$	the total area of the all stator slots [m <sup>2</sup> ]
$Q_{t1}$	the area of the stator tooth [m <sup>2</sup> ]
$\tilde{Q}_{s2}$	the area of the rotor slot [m <sup>2</sup> ]
$Q_{s2}$	the total area of the all rotor slots [m <sup>2</sup> ]
$Q_{t2}$	the area of the rotor tooth [m <sup>2</sup> ]
$k_p$	pitch factor
$k_{ew}$	radial length factor of the end winding
$k_w$	winding factor
$k_{Fe}$	space factor for iron
$k_{Cu}$	space factor for copper
$k_{Al}$	space factor for aluminum
$z_1$	the number of the stator slots
$z_2$	the number of the rotor slots
$b_{s1}$	the width of the stator slot [m]
$b_{s2}$	the width of the rotor slot [m]
$h_{s1}$	the height of the stator slot [m]
$h_{c1}$	the height of the stator core [m]
$h_{s2}$	the height of the rotor slot [m]

## References

1. Dineva, A.; Mosavi, A.; Faizollahzadeh Ardabili, S.; Vajda, I.; Shamshirband, S.; Rabczuk, T.; Chau, K.W. Review of soft computing models in design and control of rotating electrical machines. *Energies* **2019**, *12*, 1049. [\[CrossRef\]](#)
2. Virtic, P.; Pisek, P.; Marcic, T.; Hadziselimovic, M.; Stumberger, B. Analytical analysis of magnetic field and back electromotive force calculation of an axial-flux permanent magnet synchronous generator with coreless stator. *IEEE Trans. Magn.* **2008**, *44*, 4333–4336. [\[CrossRef\]](#)
3. Krasopoulos, C.T.; Beniakar, M.E.; Kladas, A.G. Multicriteria PM motor design based on ANFIS evaluation of EV driving cycle efficiency. *IEEE Trans. Transp. Electr.* **2018**, *4*, 525–535. [\[CrossRef\]](#)
4. Virtic, P.; Pisek, P.; Hadziselimovic, M.; Marcic, T.; Stumberger, B. Torque analysis of an axial flux permanent magnet synchronous machine by using analytical magnetic field calculation. *IEEE Trans. Magn.* **2009**, *45*, 1036–1039. [\[CrossRef\]](#)
5. Vrtič, P.; Vražić, M.; Papa, G. Design of an axial flux permanent magnet synchronous machine using analytical method and evolutionary optimization. *IEEE Trans. Energy Convers.* **2015**, *31*, 150–158. [\[CrossRef\]](#)

6. Muselli, M.; Notton, G.; Louche, A. Design of hybrid-photovoltaic power generator, with optimization of energy management. *Sol. Energy* **1999**, *65*, 143–157. [[CrossRef](#)]
7. Bramerdorfer, G.; Zăvoianu, A.C. Surrogate-based multi-objective optimization of electrical machine designs facilitating tolerance analysis. *IEEE Trans. Magn.* **2017**, *53*, 1–11. [[CrossRef](#)]
8. Bramerdorfer, G.; Tapia, J.A.; Pyrhönen, J.J.; Cavagnino, A. Modern electrical machine design optimization: Techniques, trends, and best practices. *IEEE Trans. Ind. Electron.* **2018**, *65*, 7672–7684. [[CrossRef](#)]
9. Meo, S.; Zohoori, A.; Vahedi, A. Optimal design of permanent magnet flux switching generator for wind applications via artificial neural network and multi-objective particle swarm optimization hybrid approach. *Energy Convers. Manag.* **2016**, *110*, 230–239. [[CrossRef](#)]
10. Hejra, M.; Mansouri, A.; Trabeisi, H. Optimal design of a permanent magnet synchronous motor: Application of in-wheel motor. In Proceedings of the 2014 5th International Renewable Energy Congress (IREC), Hammamet, Tunisia, 25–27 March 2014; pp. 1–5.
11. Raminosoa, T.; Blunier, B.; Fodorean, D.; Miraoui, A. Design and optimization of a switched reluctance motor driving a compressor for a PEM fuel-cell system for automotive applications. *IEEE Trans. Ind. Electron.* **2010**, *57*, 2988–2997. [[CrossRef](#)]
12. Knypiński, Ł.; Pawełoszek, K.; Le Menach, Y. Optimization of Low-Power Line-Start PM Motor Using Gray Wolf Metaheuristic Algorithm. *Energies* **2020**, *13*, 1186.
13. Frederico, L.S.B.F.C.; Min, G.G.J.A.R. Ant colony optimization for the topological design of interior permanent magnet (IPM) machines. *Electron. Eng.* **2014**, *26*, 1324–1345.
14. Mamede, A.C.F.; Camacho, J.R. Evolutionary algorithms for optimization of 4/4 single phase switched reluctance machine. *IEEE Lat. Am. Trans.* **2018**, *16*, 1684–1691. [[CrossRef](#)]
15. Benallal, M.; Vaganov, M.; Pantouhov, D.; Ailam, E.; Hamouda, K. Optimal value of air gap induction in an induction motor. In Proceedings of the XIX International Conference on Electrical Machines—ICEM 2010, Rome, Italy, 6–8 September 2010; pp. 1–4.
16. Pyrhonen, J.; Jokinen, T.; Hrabovcova, V. *Design of Rotating Electrical Machines*; John Wiley & Sons: Hoboken, NJ, USA, 2013.
17. Yang, Y.P.; Shih, G.Y. Optimal design of an axial-flux permanent-magnet motor for an electric vehicle based on driving scenarios. *Energies* **2016**, *9*, 285. [[CrossRef](#)]
18. Du-Bar, C. Design of an Axial Flux Machine for an In-Wheel Motor Application. Master's Thesis, Chalmers Reproservice, Göteborg, Sweden, 2011.
19. Gao, P.; Gu, Y.; Wang, X. The design of a permanent magnet in-wheel motor with dual-stator and dual-field-excitation used in electric vehicles. *Energies* **2018**, *11*, 424. [[CrossRef](#)]
20. Kreim, A.; Schäfer, U. An approach to an optimal design of permanent magnet synchronous machines for battery electric vehicles. *World Electr. Veh. J.* **2013**, *6*, 673–683. [[CrossRef](#)]
21. Nobahari, A.; Darabi, A.; Hassannia, A. Axial flux induction motor, design and evaluation of steady state modeling using equivalent circuit. In Proceedings of the 2017 8th Power Electronics, Drive Systems & Technologies Conference (PEDSTC), Mashhad, Iran, 14–16 February 2017; pp. 353–358.
22. Valtonen, M.; Parviainen, A.; Pyrhonen, J. Influence of the air-gap length to the performance of an axial-flux induction motor. In Proceedings of the 2008 18th International Conference on Electrical Machines, Vilamoura, Portugal, 6–9 September 2008; pp. 1–5.
23. Nasiri-Gheidari, Z.; Lesani, H. Design optimization of a single-phase axial flux induction motor with low torque ripple. *Przegląd Elektrotechniczny* **2012**, *88*, 168–172.